

NJC

Accepted Manuscript



This is an *Accepted Manuscript*, which has been through the Royal Society of Chemistry peer review process and has been accepted for publication.

Accepted Manuscripts are published online shortly after acceptance, before technical editing, formatting and proof reading. Using this free service, authors can make their results available to the community, in citable form, before we publish the edited article. We will replace this *Accepted Manuscript* with the edited and formatted *Advance Article* as soon as it is available.

You can find more information about *Accepted Manuscripts* in the [Information for Authors](#).

Please note that technical editing may introduce minor changes to the text and/or graphics, which may alter content. The journal's standard [Terms & Conditions](#) and the [Ethical guidelines](#) still apply. In no event shall the Royal Society of Chemistry be held responsible for any errors or omissions in this *Accepted Manuscript* or any consequences arising from the use of any information it contains.



Journal Name

ARTICLE

ESIPT and CHEF based highly sensitive and selective ratiometric sensor for Al³⁺ with imaging in human blood cell

Received 00th January 20xx,
Accepted 00th January 20xx

DOI: 10.1039/x0xx00000x

www.rsc.org/

Sangita Das,^a Shyamaprosad Goswami,^{*a} Krishnendu Aich,^a Kakali Ghoshal,^b Ching Kheng Quah,^c Maitree Bhattacharyya^b and Hoong-Kun Fun^{c,d}

Based on excited state intramolecular proton transfer (ESIPT) and chelation induced enhanced fluorescence (CHEF) mechanisms, a new fluorescence ratiometric probe for Al³⁺ was designed and synthesized and its structure was confirmed through single crystal X-ray study. This probe is capable to show excited state intramolecular proton transfer through two different pathways. Introduction of Al³⁺ in the mixed aqueous solution of the probe exhibits abrupt change in the photophysical properties. A ratiometric emission profile was noticed in presence of Al³⁺. Interestingly, the presence of other metal ions (specially trivalent ions e. g. Fe³⁺, Cr³⁺, Ga³⁺ and In³⁺) do not perturb the fluorescence intensity of the probe (except Cu²⁺ and Pb²⁺, slight changes were noticed). This indicates that the probe shows high affinity towards Al³⁺. The ratiometric sensing phenomenon may be explained as the presence of two different mechanism namely excited state intramolecular proton transfer and chelation induced enhanced fluorescence, showed by the probe in presence of Al³⁺ in the excited state. The complexation of the probe with Al³⁺ inhibits excited state intramolecular proton transfer while the chelation induced enhanced fluorescence mechanism come to play. The probe was efficient to detect the cellular uptake of Al³⁺, which is demonstrated here with human blood-cell imaging. Moreover the detection limit was found to be 6.72 × 10⁻⁸ M.

Introduction

Aluminium is well known for its wide use in daily life as it is found abundantly in nature and the third most prevalent metal in the earth's crust. Increasing proofs recommend that aluminium has inconsiderable toxicity in biological system.¹ Aluminium compounds acting as paradox in our day to day life as they are broadly used commercially in different industries like paper industry,² textile industry,³ alimentary industry^{4,5} etc, but very toxic to human life, flora, and fauna.⁶ In addition, frequent use of aluminium foil, vessels and cookie sheets in our daily life results in a reasonably increase of Al³⁺ concentration in food. Its excessive intake leads to severe health problems such as gastrointestinal ailments, Alzheimer's disease, colic, rickets, osteoporosis, anaemia, and headache etc.⁷ It can also damage the central nervous system in humans. Aluminium ions may stay for a prolonged time in various

organs and tissues before being excreted through urine. According to WHO the tolerable limit of weekly intake of Al³⁺ by human beings is around 7 mg Kg⁻¹ body weight.⁸ Sensitive bio-imaging of Al³⁺ in the cell is a requirement for understanding the fundamental mechanism about how aluminium ions cause aluminium-induced human diseases. Thus there is a great need to develop a device, enable to detect a trace level of Al³⁺ in environmental and biological samples and to control the concentration levels in the biosphere and minimize direct effects on human health. Molecular sensors are highly valuable tools for selective recognition of chemical and biological species. There are many interesting sensors reported for the detection of various analytes involving intramolecularly hydrogen bonded property, which exhibits excited state intramolecular proton transfer (ESIPT)^{9,12} through tautomerization. In the past few years, many fluorescence chemosensors have been reported for the detection of Al³⁺.¹⁰ However, most of them are typical off-on or on-off type. In this regard the sensors able to detect Al³⁺ through a ratiometric signal are seldom reported.¹¹ Ratiometric fluorescent sensors usually allow to measure the emission intensity at two different wavelengths which is beneficial for the evaluation of analytes more accurately because of its independency on the local probe concentration. In our previous works,¹² we have reported the ESIPT mechanism by using HBT (hydroxybenzothiazole) derivative, where the phenolic -OH plays the tautomerism with -N atom of benzothiazole moiety. In continuation of our work,¹³ here,

^a Department of Chemistry, Indian Institute of Engineering Science and Technology, Shibpur, Howrah-711 103, India. Fax: +91 33 2668 2916; Tel: +91 33 2668 2961-3; E-mail: spgoswamical@yahoo.com.

^b Department of Biochemistry, University of Calcutta, Kolkata – 700019, India.

^c X-ray Crystallography Unit, School of Physics, Universiti Sains Malaysia, 11800 USM, Penang, Malaysia.

^d Department of Pharmaceutical Chemistry, College of Pharmacy, King Saud University, Riyadh 11451, Saudi Arabia.

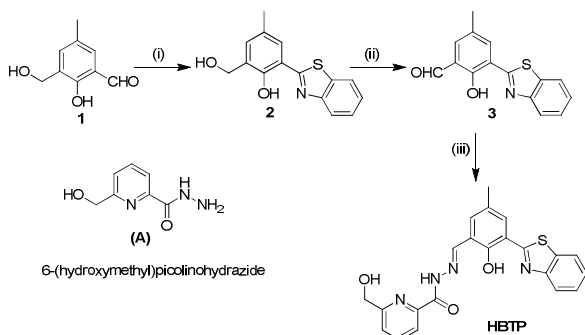
† Electronic Supplementary Information (ESI) available: [Job plot, association constant determination, detection limit determination, ¹H NMR, ¹³C NMR, ESI MS spectroscopy, fluorescence titration spectra of the receptor with different trivalent metal ions, X-ray data, Bio-imaging details, CCDC reference no. 1045374]. See DOI: 10.1039/x0xx00000x

we report the synthesis and photophysical properties of a probe (**HBTP**) (pyridine conjugated hydroxybenzothiazole) for the selective detection of Al^{3+} based on two different mechanisms (ESIPT and CHEF).

From single crystal X-ray study, it is confirmed that the probe **HBTP** shows an intramolecular hydrogen bond with phenolic –OH and hydrazide linker. Consequently in the excited state the probe may exhibit two different ESIPT by using phenolic –OH & hydrazide linker and phenolic –OH & –N atom of benzothiazole system. Introduction of Al^{3+} forms a stable complex with the probe and inhibits the ESIPT. Consequently, the chelated system exhibits a brilliant cyan emission which may be due to chelation induced enhanced fluorescence (CHEF). As per our knowledge, ESIPT and CHEF blended mechanism for the selective detection of Al^{3+} has rarely been reported. Possible practical utilization of **HBTP** as intracellular sensor of Al^{3+} was also examined by human blood cell imaging using confocal fluorescence microscope.

Results and discussion

The synthetic scheme of the probe is shown in Scheme 1. Compound 6-(hydroxymethyl)picolinohydrazide (**A**) is prepared by adopting the literature procedure, previously reported by us.¹⁴ As depicted in Scheme 1, compound **3** (3-(benzo[*d*]thiazol-2-yl)-2-hydroxy-5-methylbenzaldehyde) was treated with compound **A** to afford the final probe (**HBTP**) as light yellow solid in 81% yield. The structure of **HBTP** was confirmed by ^1H NMR, ^{13}C NMR, HRMS and single crystal X-ray study (ESI, Fig. S1–S9).



Scheme 1. Reagents and conditions: (i) 2-aminothiophenol, *p*-TSA, reflux, 6 h; (ii) MnO_2 , CHCl_3 , reflux, 12 h; (iii) 6-(hydroxymethyl)picolinohydrazide, EtOH, reflux, 3 h.

Crystallographic study of the probe (HBTP)

X-ray analysis reveals that **HBTP** crystallizes in orthorhombic system with space group *Pbca* with $a = 23.177(5)$ Å, $b = 8.5606(17)$ Å, $c = 23.924(5)$ Å, $Z = 8$ and $V = 4746.9(17)$ Å³. A summary of crystal data and parameters for structure refinement details are given in Table S1 (ESI) whereas the hydrogen-bond geometry can be found in Table S2 (ESI). The asymmetric unit (Fig. 1) comprises a **HBTP** and a dimethyl sulfoxide solvent molecule. The C12—C14—N2—N3 torsion angle of $179.9(3)^\circ$ involving the N2 = C14 (bond length = $1.283(5)$ Å) double bond supports the (*E*)-configuration of the structure. In **HBTP**, the mean plane of benzo[*d*]thiazole ring

system (S1/N1/C1–C7, *r.m.s.* deviation = 0.005 Å) forms dihedral angles of $8.58(16)$ and $7.64(17)^\circ$ with the benzene (C8–C13) and pyridine (N4/C16–C20) rings, indicating they are almost coplanar to each other. The dihedral angle between benzene and pyridine rings is $1.49(19)^\circ$. The crystal structure features for intramolecular O—H \cdots N hydrogen bond producing an *S*(6) ring motif, which is assumed to contribute to the stability of the molecule. In the crystal packing (Figure S10, ESI), the **HBTP** molecules are connected to the solvent molecule *via* intermolecular O3—H1O3 \cdots O4, N3—H1N3 \cdots O4 and C14—H14A \cdots S2 (Table S2, ESI) hydrogen bonds and are stacked along [010], result in the formation of $R_2^1(10)$ and $R_2^2(7)$ ring motifs. The molecular packing is stabilized by weak C—H \cdots π interactions involving the centroid of the C1–C6 benzene ring.

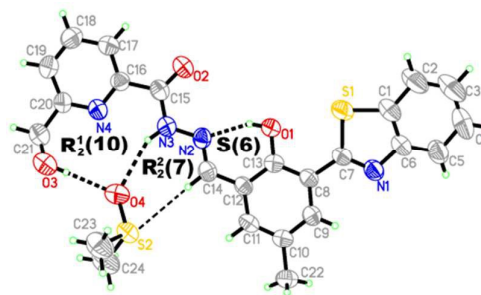


Figure 1 The molecular structure of the probe (**HBTP**), showing 50% probability displacement ellipsoids for non-H atoms and the atom-numbering scheme. Hydrogen bonds are represented by dashed lines.

Sensing of Al^{3+} by UV-vis method

To examine the selectivity of **HBTP**, UV-vis and fluorescence titration experiments were performed using common interfering analytes (Na^+ , K^+ , Ca^{2+} , Ni^{2+} , Mn^{2+} , Zn^{2+} , Cd^{2+} , Ga^{3+} , Cu^{2+} , Fe^{3+} , Cr^{3+} , Pb^{2+} , In^{3+} , Hg^{2+} and Al^{3+} in $\text{H}_2\text{O}/\text{MeOH}$ (9/1, v/v, 10 mM PBS buffer, pH = 7.3, 25°C) solution. The changes in absorption spectra during the Al^{3+} titration have shown in Fig. 2a. **HBTP** (10 μM) itself showed two peaks at 270 nm and 370 nm in the absorbance profile.

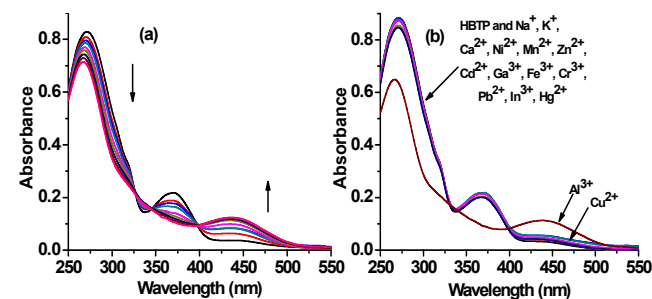


Figure 2 (a) Absorption spectra of **HBTP** (10 μM) upon titration with Al^{3+} (0 to 2 equivalents) in $\text{CH}_3\text{OH}/\text{H}_2\text{O}$ (1/9, v/v, pH = 7.3, 25°C) solution. (b) Changes of absorption spectra of **HBTP** (10 μM) upon addition of different cations (5 equivalents).

Upon addition of increasing concentrations of Al^{3+} (0–2 equiv.) the first two bands around 270 nm and 370 nm got decreased regularly and a new peak at 440 nm gradually increases. Only Al^{3+} has been successful to perturb the absorption signal of

HBTP but other analytes cannot affect the absorption profile in a significant extent (Cu^{2+} showed slight interference) (Fig. 2b). It has been observed that the absorbance intensity at 440 nm exhibits a good linear relationship with added Al^{3+} concentration from 0 to 10 μM , after that plateau was reached, indicates the saturation takes place. In the presence of Al^{3+} ion, the color of the solution of HBTP changes from colourless to light yellow. The association constant for the Al^{3+} complexation with **HBTP** was estimated to be $1.24 \times 10^5 \text{ M}^{-1}$ from Benesi-Hildebrand plot¹⁵ using the data obtained from UV-vis titration (Fig. S11, ESI).

Sensing of Al^{3+} by fluorescence method

The metal binding ability of the probe (**HBTP**) was evaluated by fluorescence spectral analysis. Herein we have elaborated the fluorogenic signalling behaviour of **HBTP** (10 μM) in $\text{CH}_3\text{OH}/\text{H}_2\text{O}$ (1/9, v/v, and pH = 7.3, 10 mM PBS buffer, 25°C) solution towards the detection of Al^{3+} . Fig. 3a shows the fluorescence spectrum of the probe (**HBTP**) in the presence of 2 equiv. of Al^{3+} . Free probe displayed two broad bands at 435 nm and 565 nm. Upon incremental addition of Al^{3+} ion (0-2 equiv.) the peak at 565 nm decreased whereas a new band at 480 nm increases rapidly. Upon addition of almost two equivalents of Al^{3+} , the intensity at 480 nm increased by almost 25 times than that of the probe itself. Consequently, a prominent fluorescence colour change was observed from red to cyan (Fig. 3a, inset). The changes in the fluorescence spectra stopped when the amount of added Al^{3+} reached 1.2 equivalents. A good linear relationship was observed between the ratio of fluorescence intensities (I_{480}/I_{565}) and concentration of added Al^{3+} (0 – 12 μM , Fig. S12, ESI). The detection limit of the probe for Al^{3+} was determined from the fluorescence spectral change, and it was found to be $6.72 \times 10^{-8} \text{ M}$, using the equation $\text{DL} = K \times \text{Sb}_1/\text{S}$, where $K = 3$, Sb_1 is the standard deviation of the blank solution and S is the slope of the calibration curve¹⁶ (Fig. S12, ESI). Notably, addition of other co-existing analytes, even in excess amount, caused insignificant change in the emission intensity of the probe (Fig. 3b). Especially no other trivalent ions (e.g. Fe^{3+} , Cr^{3+} , Ga^{3+} and In^{3+}) can cause a considerable change in the fluorescence profile of the probe (Fig. S23, ESI).

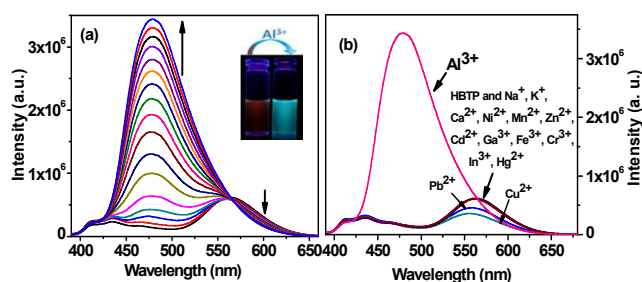


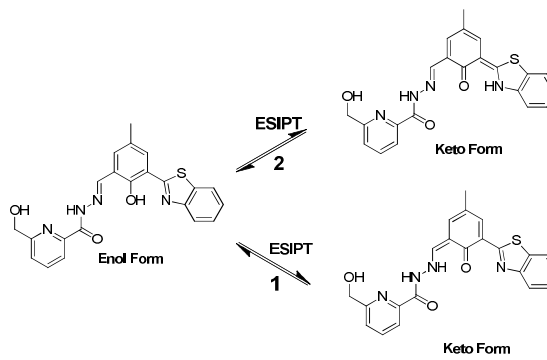
Figure 3 (a) Fluorescence spectra of HBTP (10 μM) upon titration with Al^{3+} (0 to 2 equivalents) in $\text{CH}_3\text{OH}/\text{H}_2\text{O}$ (1/9, v/v, pH = 7.3, 25°C) solution. Inset: Emission colour change of HBTP upon addition of 2 equivalents of Al^{3+} after illumination under UV light. (b) Emission spectra of HBTP (10 μM) upon addition of different metal ions (5 equivalents). $\lambda_{\text{exc}} = 380 \text{ nm}$.

In case of Cu^{2+} and Pb^{2+} a slight quench of fluorescence intensity at 565 nm was noticed with no interference at 480 nm. Figure S15 (ESI) shows a comparative view of emission intensity of the probe **HBTP** after adding 3.0 equiv. of each of the guest analytes in presence of Al^{3+} . This indicates with background of most selected coexistent metal ions does not interfere the sensing of **HBTP** for Al^{3+} . A comparison of the present probe with recently reported probes for Al^{3+} have been outlined in Table S4 (ESI).

We have performed the fluorescence titration of the probe with Al^{3+} in different solvent systems like DMSO only, ethanol/water (1/9) and DMSO/water (2/98) and results are given in the ESI (Fig. S20 – S22). The results were almost similar to that of methanol-water system (Fig. 3a).

Sensing mechanism of the probe with Al^{3+}

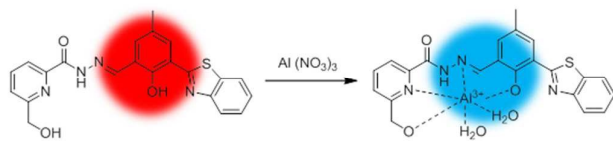
The two-way ESIPT of the free probe (**HBTP**) was given in scheme 2, where the equilibrium 1 is predominant over equilibrium 2. From single crystal X-ray study, it is confirmed the existence of intramolecular hydrogen bond between phenolic –OH and hydrazide linker, this explains the predominance of equilibrium 1 in the free probe. The change in colour of fluorescence after introduction of Al^{3+} was observed mainly due to the inhibition of ESIPT. As from the HSAB concept Al^{3+} being a hard acid loves to bind with hard centers, like oxygen atom of the ethanol moiety, nitrogen atom of the pyridyl moiety, hydrazide nitrogen atom and oxygen of phenolic –OH group. The guest analyte Al^{3+} prone to bind in this site, thus ESIPT stops and CHEF plays the key role resulting cyan emission. Because of the isomerization in the imine segment ($-\text{C}=\text{N}$), the probe may take any conformation, either 'E' or 'Z'. Consequently, the probe is more flexible in this situation. But after addition of Al^{3+} , restriction in the flexibility is being employed and the complex become rigid and this may also plays the key role for the enhancement in fluorescence.



Scheme 2: Probable two-way ESIPT of the probe HBTP

The complexation of the probe with Al^{3+} (Scheme 3) was confirmed through ^1H NMR titration study (Fig. S16, ESI). The ^1H NMR titration study clear the unavailability of –OH proton in $\text{HBTP}-\text{Al}^{3+}$ (the peak of phenolic –OH at $\delta = 13.28 \text{ ppm}$ gradually vanished after addition of 1 equivalent Al^{3+}),

indicates that the phenolic proton may take part in complexation with Al^{3+} .



Scheme 3. Probable binding mode of the probe with Al^{3+}

Now no peak at $\delta = 5.56$ ppm, also indicates the lack of aliphatic $-\text{OH}$ proton of the pyridine ring, this observation showed that Al^{3+} chose to bind with the hard aliphatic oxygen atom, confirm the complexation of Al^{3+} using this binding sight. The ^1H NMR titration study not only established the fact that Al^{3+} plays as the key to lock ESIPT and favours CHEF but also explains the exact binding site. The HRMS spectra of $\text{HBTP}-\text{Al}^{3+}$ showed a peak at 479.0174 which may be for $[\text{M}+\text{Al}^{3+}+2\text{H}_2\text{O}-2\text{H}^+]^+$ (Fig. S17, ESI, Scheme 3). The IR spectra were recorded for **HBTP** and $\text{HBTP}-\text{Al}^{3+}$ complex which were given in Fig. S24 (ESI) also supported the complex formation. Depending on the above findings we may conclude the probable complex structure of $\text{HBTP}-\text{Al}^{3+}$ and is given in Scheme 3.

The Job's plot analysis was performed in order to establish the exact stoichiometry of the complexation. In this experiment we have recorded the change in emission at 480 nm against molar fractions of **HBTP** and Al^{3+} under the conditions of an invariant total concentration. The maximum point appears at mole fraction of 0.5, which corresponds to a 1:1 (host-guest) complex formation of **HBTP** and Al^{3+} (Fig S14, ESI).

pH dependency of the probe and its complex with Al^{3+}

In order to investigate the response of the probe towards different pH, we have recorded the fluorescence spectra of **HBTP** at different pH solutions (Fig. S18a, ESI). It was observed that **HBTP** was almost nonresponsive within pH range 3-9. But with increasing pH (10-12), a slight enhancement was noticed at 480 nm. Now from the above experiment, it was concluded that our probe is stable in biological pH, so that intracellular experiment can be performed by it. The pH sensitivity of **HBTP** in presence of Al^{3+} was also studied. The detection of Al^{3+} was not affected within the pH range from pH = 1.2 to pH = 9, but with increasing pH (> 10) the detection of Al^{3+} was a little bit hampered. The pH study revealed that the probe **HBTP** can detect Al^{3+} with no such interference in acidic, near neutral and moderate basic pH conditions (Fig. S18b, ESI).

Live-cells imaging and cytotoxic effect of the probe and its Al^{3+} complex

HBTP is particularly useful for imaging of biological samples for its permeability as well as stability in neutral pH. This fluorescent probe is easily taken up by the cells without causing any damages such as lysis or swelling. Cell viability

assay was also performed with the probe in presence and absence of Al^{3+} ; it was given in figure S19 (ESI). This experiment shows that **HBTP** is non-toxic to living cells. Fig. 4a depicts the bioimaging of human PBMCs by **HBTP** when there is no added Al^{3+} from outside. Here cells have shown significant red fluorescence and very little or no green fluorescence. Fig. 4d surprisingly shows a far greater green intensity indicating the interactions between **HBTP** and Al^{3+} . Average fluorescence intensity has been calculated by Olympus Fluoview FV 1000 software and results have been given in Table S3 (ESI). The green/red ratio is significantly lower in samples without added Al^{3+} (0.046) where its value is far higher (6.2) when externally Al^{3+} is being added. The green/red fluorescence ratios implicate the shifting of green fluorescence from red fluorescence by externally added Al^{3+} . Thus, **HBTP** has been proven to be a successful probe for bioimaging.

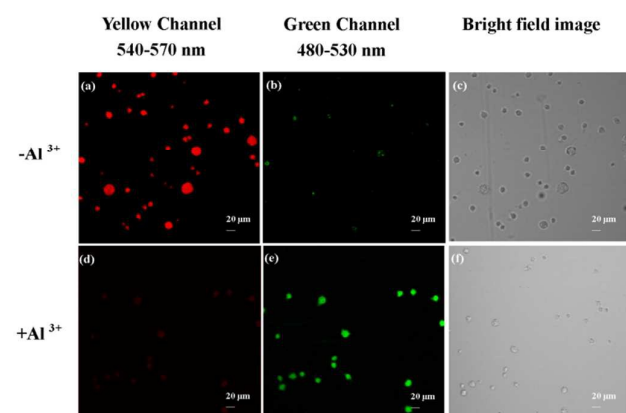


Figure 4 Confocal fluorescence images (60X) of human PBMCs treated with 10 μM **HBTP** (a & b) and then the same was treated with 10 μM Al^{3+} solution (d & e) respectively. Images were taken from (a & d) yellow channel (540 nm – 570 nm) and (b & e) green channel (480 nm – 530 nm). λ_{exc} = 400 nm. Larger cells are macrophages in PBMC populations. C & f are the bright-field images of the cells with probe before and after addition of Al^{3+} respectively.

Conclusions

In summary, we report here the design, synthesis and cation sensing property of a new hydroxybenzothiazole-pyridine based probe. It showed highly selective and sensitive response to Al^{3+} over other competing metal cations in MeOH/ H_2O (1/9, v/v, pH = 7.3, 10 mM PBS buffer, 25°C) media. A large enhancement of ratiometric emission intensity was observed after introduction of Al^{3+} . The detection limit was found to be 10^{-8} M level, which indicates our probe (**HBTP**) is a highly efficient sensor of Al^{3+} in mixed aqueous media. The introduction of Al^{3+} in the solution of the probe (**HBTP**) stops excited state intramolecular proton transfer and 'turns on' the chelation induced enhanced fluorescence mechanism. Other cations do not hamper the detection Al^{3+} in a significant extent. The probe can also be used in human blood cell imaging.

Experimental

General

The materials used for this study were obtained from Sigma-Aldrich and used without further purification. Merck 60 F₂₅₄ plates with a thickness of 0.25 mm were used for thin layer chromatography (TLC). ¹H and ¹³C NMR spectra were recorded on Bruker 400 MHz and 100 MHz instruments and mentioned in the figure captions of the NMR spectra. CDCl₃ or DMSO-d₆ were used as solvent for NMR spectra using TMS as an internal standard. UV-vis spectra were recorded on a JASCO V-630 spectrometer. Fluorescence spectra were recorded on PTI (Photon Technology International) fluorescence spectrometer. For the titration experiment we used the cations (metal ions) viz. [Na⁺, K⁺, Ca²⁺, Ni²⁺, Mn²⁺, Zn²⁺, Cd²⁺, Cu²⁺, Fe³⁺, Mg²⁺, Cr³⁺ and Pb²⁺] as their chloride salts and Al³⁺ as its nitrate salt.

General method of UV-vis and fluorescence titration

UV-vis method

For UV-vis titrations, stock solution of the receptor (10 μM) was prepared in [(CH₃OH / water), 1/9, v/v] (at 25°C) using PBS buffered solution. The solutions of the guest cations using their chloride salts in the order of 1 × 10⁻⁵ M, were prepared in deionized water using PBS buffer at pH = 7.3. Solutions of various concentrations containing the sensor and increasing concentrations of cations were prepared separately. The spectra of these solutions were recorded by means of UV-vis method.

Fluorescence method

For fluorescence titrations, stock solution of the sensor (10 μM) used was the same as that used for UV-vis titration. The solutions of the guest cations using their chloride salts in the order of 1 × 10⁻⁵ M, were prepared in deionised water. Solutions of various concentrations containing sensor and increasing concentrations of cations were prepared separately. The spectra of these solutions were recorded by means of fluorescence method.

Determination of fluorescence quantum yield

To determine the quantum yields of HBTP and HBTP-Al³⁺, we recorded their absorbance in methanol solution. The emission spectra were recorded using the maximal excitation wavelengths, and the integrated areas of the fluorescence-corrected spectra were measured. The quantum yields were then calculated by comparison with fluorescein (Φ_s = 0.97 in basic ethanol) as reference using the following equation:

$$\Phi_x = \Phi_s \times (I_x/I_s) \times (A_s/A_x) \times (n_x/n_s)^2$$

where, x & s indicate the unknown and standard solutions respectively, Φ is the quantum yield, I is the integrated area under the fluorescence spectra, A is the absorbance and n is the refractive index of the solvent.

We calculated the quantum yields of HBTP and HBTP-Al³⁺ using the above equation and the values are 0.087 and 0.46 respectively.

Synthetic method for the preparation of the probe

Synthesis of compound 2

To the suspension of 1 [2-hydroxy-3-(hydroxymethyl)-5-methylbenzaldehyde] (0.5 g, 3.01 mmol) in ethanol (10 ml), 2-

aminothiophenol (0.45 g, 3.6 mmol) was added with continuous stirring under the N₂-atmosphere. A catalytic amount of p-TSA (10 mg) was added to it and the reaction mixture was refluxed for 6 hours. After that, the solvents were evaporated under reduced pressure and the crude solid was purified on a silica gel column chromatography using 5-10% ethyl acetate in petroleum ether (v/v) as the eluant. The product was obtained as light yellow solid. Yield = (0.65 g) 80%.

¹H NMR (500 MHz, CDCl₃): δ 2.36 (s, 3H), 4.80 (s, 2H), 7.22 (s, 1H), 7.43 (m, 2H), 7.51 (t, J = 7.7 Hz, 1H), 7.91 (d, J = 8 Hz, 1H), 7.98 (d, J = 8 Hz, 1H).

HRMS (ESI, positive): calcd. for C₁₅H₁₃NNaO₂S [M + Na]⁺ (m/z): 294.0565; found: 294.0566.

Synthesis of compound 3

MnO₂ (0.26 g, 2.98 mmol) was added to a solution of 2 (0.4 g, 1.47 mmol) in chloroform (30 ml) under the N₂-atmosphere. Then the mixture was heated to reflux for 12 hours. The reaction mixture was then passed through a celite bed (5 cm) and to evaporate the solvent. The solid residues were collected and purified on a silica gel column using ethyl acetate in petroleum ether (1/4, v/v) as eluent. Compound 3 was obtained as white solid. Yield = (0.28 g) 70%.

¹H NMR (500 MHz, CDCl₃): δ 2.44 (s, 3H), 7.47 (t, J = 7.5 Hz, 1H), 7.57 (t, J = 7.5 Hz, 1H), 7.72 (s, 1H), 7.95 (d, J = 8 Hz, 1H), 8.14 (d, J = 8 Hz, 2H), 10.42 (s, 1H).

HRMS (ESI, positive): calcd. for C₁₅H₁₁NNaO₂S [M + Na]⁺ (m/z): 292.0408; found: 292.0405.

Synthesis of the probe (HBTP)

6-(hydroxymethyl)picolinohydrazide (0.2 g, 1.19 mmol) was added to a solution of 3 (0.32 g, 1.19 mmol) in ethanol (10 ml). After addition, the reaction mixture was refluxed for 3 hours and then cooled to room temperature. Yellowish-white precipitate obtained was filtered and washed with cold ethanol (2 × 2 ml). Yield = (0.4 g) 82%.

¹H NMR (500 MHz, DMSO-d₆): δ 2.39 (s, 3H), 4.74 (s, 2H), 5.56 (s, 1H), 7.46 (t, J = 7 Hz, 1H), 7.55 (t, J = 6.5 Hz, 2H), 7.72 (d, J = 7.5 Hz, 1H), 8.04 (m, 3H), 8.16 (m, 2H), 8.90 (s, 1H), 12.45 (s, 1H), 13.28 (s, 1H).

¹³C NMR (125 MHz, DMSO-d₆): δ 19.8, 63.8, 119.4, 119.5, 120.9, 121.9, 122.2, 123.7, 125.0, 126.4, 128.6, 130.5, 132.9, 134.7, 138.3, 147.8, 149.2, 151.3, 154.0, 160.4, 161.0, 163.3

HRMS (ESI, positive): calcd. for C₂₂H₁₈N₄NaO₃S [M + Na]⁺ (m/z): 441.0997; found: 441.0996.

Method of crystallization

An amount of 20 mg of HBTP was dissolved in a small conical in DCM/DMSO (1/1, v/v) solution. Then the conical was placed gently in a cool place without any perturbation. After five days, yellow crystals were obtained.

Synthesis of Al³⁺ complex (HBTP-Al³⁺) of receptor

The receptor, HBTP (50 mg) and Al(NO₃)₃ (14 mg) were mixed together and dissolved in 5 ml of methanol. After reflux for 12 hours the reaction mixture was cooled to room temperature. A reddish-yellow coloured precipitate appeared which was filtered and dried in vacuum.

HRMS (ESI, Positive): calcd. for C₂₂H₂₀AlN₄O₅S [M + Al³⁺ + 2H₂O-2H⁺]⁺ (m/z): 479.0953; found: 479.0174.

Details of live-cell imaging**Materials Methods**

3 ml of venous blood was obtained from volunteer donor (age \geq 30 years) with his informed consent. Peripheral blood mononuclear cells (PBMCs) were isolated by density gradient centrifugation by histopaque-1077 obtained by SIGMA. PBMCs were washed and suspended in PBS and were divided in two sets. In one set, 10 μ M Al(NO₃)₃ solution was added as a source of Al³⁺. Another set was devoid of any externally added Al³⁺. **HBTP** samples were prepared in PBS containing 0.5% DMSO. Both the samples were incubated with 10 μ M **HBTP** solutions for 15 minutes at 37°C. Cells were observed under confocal fluorescence microscope (Olympus IX81 microscope) with fluorescence emissions at 480 nm and 560 nm, respectively.

Acknowledgements

Authors thank CSIR and DST, Govt. of India for financial supports. S.D, K.A and K.G acknowledge CSIR for providing them fellowship. CKQ and HKF thank Universiti Sains Malaysia for Research University Individual Grant (No. 1001/PFIZIK/811278). The authors extend their appreciation to The Deanship of Scientific Research at King Saud University for the research group project No. RGP VPP-207.

Notes and references

- (a) T. P. Flaten, M. Ødegård, *Food Chem. Toxicol.*, 1988, **26**, 959; (b) J. Ren, H. Tian, *Sensors*, 2007, **7**, 3166; (c) Yokel, R. A. *Neurotoxicology*, 2000, **21**, 813.
- W. S. Miller, L. Zhuang, J. Bottema, A. J. Wittebrood, P. De Smet, A. Haszler and A. Vieregge, *Mater. Sci. Eng., A*, 2000, **280**, 37.
- G. Ciardelli and N. Ranieri, *Water Res.*, 2001, **35**, 567.
- S. Humphreys, P. M. Bolger, P. F. Zatta and A.C. Alfrey, (Eds.), *A Public Health Analysis of Dietary Aluminium*, World Scientific, Singapore, 1997, 226.
- R. A. Yokel, *Food Chem. Toxicol.*, 2008, **46**, 2261.
- (a) E. Delhaize and P. R. Ryan, *Plant Physiol.*, 1995, **107**, 315; (b) D. L. Godbold, E. Fritz and A. Huttermann, *Proc. Natl. Acad. Sci. USA*, 1988, **85**, 3888.
- G. Berthon, *Coord. Chem. Rev.*, 2002, **228**, 319; (b) T. P. Flaten, *Brain Res. Bull.*, 2001, **55**, 187.
- (a) J. Barcelo and C. Poschenrieder, *Environ. Exp. Bot.*, 2002, **48**, 75; (b) Z. Krejpcio and R. W. P. Wojciak, *J. Environ. Studies*, 2002, **11**, 251.
- (a) Z. Xu, L. Xu, J. Zhou, Y. Xu, W. Zhu and X. Qian, *Chem. Commun.*, 2012, **48**, 10871; (b) M. Santra, B. Roy, K. H. Ahn, *Org. Lett.*, 2011, **13**, 3422; (c) D. Maity, V. Kumar, T. Govindaraju, *Org. Lett.*, 2012, **14**, 6008; (d) Z. Song, R. T. K. Kwok, E. Zhao, Z. He, Y. Hong, J. W. Y. Lam, B. Liu, and B. Z. Tang, *ACS Appl. Mater. Interfaces*, 2014, **6**, 17245; (e) L. Tang, Z. Zheng, Z. Huang, K. Zhong, Y. Biana and R. Nandhakumar, *RSC Adv.*, 2015, **5**, 10505; (f) L. Tang, M. Cai, P. Zhou, J. Zhao, K. Zhong, S. Hou and Y. Bian, *RSC Adv.*, 2013, **3**, 16802; (g) L. Tang, X. Dai, K. Zhong, D. Wu and X. Wen, *Sensors and Actuators B*, 2014, **203**, 557.
- (a) D. Maity and T. Govindaraju, *Inorg. Chem.*, 2010, **49**, 7229; (b) A. Sahana, A. Banerjee, S. Das, S. Lohar, D. Karak, B. Sarkar, S. K. Mukhopadhyay, A. K. Mukherjee and D. Das, *Org. Biomol. Chem.*, 2011, **9**, 5523; (c) A. Banerjee, A. Sahana, S. Das, S. Lohar, S. Guha, B. Sarkar, S. K. Mukhopadhyay, A. K. Mukherjee and D. Das, *Analyst*, 2012, **137**, 2166; (d) S. Goswami, K. Aich, S. Das, A. K. Das, D. Sarkar, S. Panja, T. K. Mondal and S. Mukhopadhyay, *Chem. Commun.*, 2013, **49**, 10739; (e) Y. Lu, S. Huang, Y. Liu, S. He, L. Zhao and X. Zeng, *Org. Lett.*, 2011, **13**, 5274; (f) K. K. Upadhyay, and A. Kumar, *Org. Biomol. Chem.*, 2010, **8**, 4892; (g) S. Samanta, S. Goswami, Md. N. Hoque, A. Ramesh and G. Das, *Chem. Commun.*, 2014, **50**, 11833; (h) S. Goswami, K. Aich, A. K. Das, and S. Das, *RSC Adv.*, 2013, **3**, 2412.
- (a) D. Maity and T. Gobindoraju, *Chem. Commun.*, 2012, **48**, 1039; (b) X. Sun, Y.-W. Wang and Y. Peng, *Org. Lett.*, 2012, **14**, 3420; (c) A. Sahana, A. Banerjee, S. Lohar, B. Sarkar, S. K. Mukhopadhyay and D. Das, *Inorg. Chem.*, 2013, **52**, 3627.
- (a) S. Goswami, S. Das, K. Aich, B. Pakhira, S. Panja, S. K. Mukherjee and S. Sarkar, *Org. Lett.*, 2013, **15**, 5412; (b) S. Goswami, A. Manna, S. Paul, A. K. Das, K. Aich and P. K. Nandi, *Chem. Commun.*, 2013, **49**, 2912.
- (a) S. Goswami, K. Aich, S. Das, S. B. Roy, B. Pakhira and S. Sarkar, *RSC Adv.*, 2014, **4**, 14210; (b) S. Goswami, S. Das, K. Aich, P. K. Nandi, K. Ghoshal, C. K. Quah, M. Bhattacharyya, H.-K. Fun and H. A. Abdel-Aziz, *RSC Adv.*, 2014, **4**, 24881; (c) S. Goswami, K. Aich, S. Das, A. K. Das, A. Manna and S. Halder, *Analyst*, 2013, **138**, 1903; (d) S. Goswami, S. Das, K. Aich, D. Sarkar and T. K. Mondal, *Tetrahedron Lett.*, 2014, **55**, 2695; (e) S. Goswami, S. Das and K. Aich, *Tetrahedron Lett.*, 2013, **54**, 4620; (f) S. Goswami, K. Aich, S. Das, D. Sarkar, C. D. Mukhopadhyay, D. Sarkar and T.K. Mondal, *Dalton Trans.*, 2015, **44**, 5763; (g) S. Goswami, S. Das and K. Aich, *RSC Adv.*, 2015, **5**, 28996; (h) S. Goswami, K. Aich, S. Das, B. Pakhira, K. Ghoshal, C. K. Quah, M. Bhattacharyya, H.-K. Fun and S. Sarkar, *Chem. Asian J.*, 2015, **10**, 694; (i) S. Goswami, S. Das, K. Aich, D. Sarkar and T.K. Mondal, *Tetrahedron Lett.*, 2014, **55**, 2695; (j) K. Aich, S. Goswami, S. Das, C. D. Mukhopadhyay, C. K. Quah, and H.-K. Fun, *Inorg. Chem.*, 2015, DOI: 10.1021/acs.inorgchem.5b00784.
- S. Goswami, S. Das, K. Aich, D. Sarkar, T. K. Mondal, C. K. Quah and H.-K. Fun, *Dalton Trans.*, 2013, **42**, 15113.
- (a) H. A. Benesi and J. H. Hildebrand, *J. Am. Chem. Soc.*, 1949, **71**, 2703; (b) D. C. Carter and J. X. Ho, *Adv. Protein Chem.*, 1994, **45**, 153; (c) A. Mallick and N. Chattopadhyay, *Photochem. Photobiol.*, 2005, **81**, 419; (d) I. Ravikumar, B. N. Ahamed and P. Ghosh, *Tetrahedron*, 2007, **63**, 12940.
- (a) M. Shortreed, R. Kopelman, M. Kuhn and B. Hoyland, *Anal. Chem.*, 1996, **68**, 1414; (b) W. Lin, L. Yuan, Z. Cao, Y. Feng and L. Long, *Chem.–Eur. J.*, 2009, **15**, 5096.

Graphical abstract:

We have synthesised a probe for fluorescence ratiometric detection of Al^{3+} . The probe can image Al^{3+} in living cells.

